AGU PUBLICATIONS

Geophysical Research Letters

RESEARCH LETTER

10.1002/2014GL061738

Key Points:

- CMIP5 ozone data set is at the lower end of observed depletion for ozone hole region
- Using upper estimate of depletion doubles stratospheric signal of ozone hole and increases tropospheric signal of the ozone hole by 20–100%

Correspondence to:
P. J. Young,
paul.j.young@lancaster.ac.uk

Citation:
Young, P. J., S. M. Davis, B. Hassler, S. Solomon, and K. H. Rosenlof (2014), Modeling the climate impact of Southern Hemisphere ozone depletion: The importance of the ozone data set, *Geophys. Res. Lett.*, *41*, 9033–9039, doi:10.1002/2014GL061738.

Received 1 SEP 2014
Accepted 13 NOV 2014
Accepted article online 18 NOV 2014
Published online 16 DEC 2014

Modeling the climate impact of Southern Hemisphere ozone depletion: The importance of the ozone data set

P. J. Young[1], S. M. Davis[2,3], B. Hassler[2,3], S. Solomon[4], and K. H. Rosenlof[3]

[1]Lancaster Environment Centre, Lancaster University, Lancaster, UK, [2]Cooperative Institute for Research in Environmental Sciences, University of Colorado, Boulder, Colorado, USA, [3]NOAA Earth System Research Laboratory, Boulder, Colorado, USA, [4]Department of Earth, Atmospheric, and Planetary Sciences, Massachusetts Institute of Technology, Cambridge, Massachusetts, USA

Abstract The ozone hole is an important driver of recent Southern Hemisphere (SH) climate change, and capturing these changes is a goal of climate modeling. Most climate models are driven by off-line ozone data sets. Previous studies have shown that there is a substantial range in estimates of SH ozone depletion, but the implications of this range have not been examined systematically. We use a climate model to evaluate the difference between using the ozone forcing (Stratospheric Processes and their Role in Climate (SPARC)) used by many Intergovernmental Panel on Climate Change Fifth Assessment Report (Coupled Model Intercomparison Project) models and one at the upper end of the observed depletion estimates (Binary Database of Profiles (BDBP)). In the stratosphere, we find that austral spring/summer polar cap cooling, geopotential height decreases, and zonal wind increases in the BDBP simulations are all doubled compared to the SPARC simulations, while tropospheric responses are 20–100% larger. These results are important for studies attempting to diagnose the climate fingerprints of ozone depletion.

1. Introduction

The austral spring depletion of Antarctic stratospheric ozone (the ozone hole) has emerged as one of the largest signals of global environmental change over the twentieth century, with impacts on stratospheric temperatures [*Randel et al.*, 2009], surface UV [*Mckenzie et al.*, 2011], and tropospheric climate [*Thompson et al.*, 2011]. The tropospheric climate impact of the ozone hole appears to be mediated through a trend toward a positive index of the Southern Annular Mode (SAM) during austral summer, leading to a poleward shift of the Southern Hemisphere (SH) storm tracks and other circulation shifts which stretch into the tropics [*Thompson et al.*, 2011]. The ozone depletion/SAM connection was first documented in observations by *Thompson and Solomon* [2002], and several climate model studies have since demonstrated the need to include a representation of stratospheric ozone depletion in order to capture the observed SAM trends [e.g., *Gillett and Thompson*, 2003; *Son et al.*, 2009]. Moreover, *Polvani et al.* [2011] suggested that the ozone hole was the dominant driver of twentieth century summertime SH circulation changes, and *Kang et al.* [2011] showed how the impacts extend to SH subtropical precipitation. The present study revisits the SH ozone/climate links through model simulations forced with different ozone depletion levels, with the aim of exploring the sensitivity of the stratospheric and tropospheric climate responses to varying the magnitude of the ozone hole within the range of observational uncertainty.

Despite increases in the complexity of global climate models, many do not include online representations of atmospheric chemistry and instead rely on off-line data sets. For example, 28 out of the 46 climate models submitting simulations for the Fifth Coupled Model Intercomparison Project (CMIP5) [*Taylor et al.*, 2012] were forced with an off-line data set [*Eyring et al.*, 2013]. Of these 28 models, 22 used the SPARC (Stratospheric Processes and their Role in Climate) ozone data set [*Cionni et al.*, 2011], which is similar to the data set of *Randel and Wu* [2007] for 1979–2009 and which does not capture the lowest ozone values reported over Antarctica [*Bodeker et al.*, 2013; *Hassler et al.*, 2013]. Since the magnitude of ozone depletion is thought to be related to the strength of modeled climate changes (such as temperature and jet position) [e.g., *Eyring et al.*, 2013; *Young et al.*, 2013a], there is the potential for simulations using the SPARC ozone data set to underestimate the contribution of ozone depletion to historical climate changes. Estimating this contribution is central to attribution studies [e.g., *Gillett et al.*, 2011; *Gerber and Son*, 2014], including understanding

whether Antarctic ozone depletion has been the driver behind recent regional climate changes in, for example, Africa [*Manatsa et al*., 2013] and South America [*Gonzalez et al*., 2013]. More recently, stratospheric ozone levels have been shown to have some predictive potential at seasonal time scales [*Son et al*., 2013; *Bandoro et al*., 2014; *Seviour et al*., 2014], underlining the importance of more accurate ozone concentrations in atmospheric models.

In this study, we compare model simulations forced with ozone depletion from the SPARC data set and from the Binary Database of Profiles (BDBP) data set [*Bodeker et al*., 2013], which has a more severe ozone hole [*Hassler et al*., 2013]. The primary purpose is to estimate the different atmospheric responses to ozone depletion from the two data sets. We find that the larger Antarctic ozone depletion in the BDBP data set results in significantly stronger climate responses in the stratosphere, leading to stronger changes in the troposphere. We also discuss our results in the context of the CMIP5 simulations forced by the SPARC ozone data set.

2. CAM and CMIP5 Model Simulations

The model simulations conducted for this study are the same as reported previously by *Solomon et al.* [2012], using version 3 of the Community Atmosphere Model (CAM) [*Collins et al*., 2006], which has a horizontal resolution of 1.9°×2.5° (latitude/longitude) and 26 vertical levels, from the surface to ~3.5 hPa. Briefly, two pairs of 100 year time slice simulations were conducted, with one pair using the SPARC ozone data set [*Cionni et al*., 2011] and the other pair using the BDBP data set [*Bodeker et al*., 2013]. Each pair consists of one simulation forced by ozone concentrations averaged for 1979–1981 ("preozone hole") and one simulation with ozone concentrations averaged for 1995–1997 ("ozone hole"). All other climate forcings—sea surface temperatures, sea ice concentrations, and greenhouse gas concentrations—were identical in the four simulations, set at late twentieth century climatological values. Furthermore, ozone changes were restricted to the stratosphere, and any tropospheric ozone changes over the period [*Shindell et al*., 2013; *Young et al*., 2013b] were ignored, with each simulation using the same tropospheric ozone climatology [*Logan*, 1999] imposed below a climatological, seasonally varying tropopause. As is common in model studies, both ozone data sets are monthly and zonally averaged and therefore ignore any potential climate impact of a zonally asymmetric ozone field [*Gillett et al*., 2009].

We consider ozone concentrations over 1979–1997 as this is generally the first period used when fitting piecewise linear trends to Antarctic austral spring ozone concentrations, with the trend becoming less negative after this time [*Reinsel et al*., 2002; *Chehade et al*., 2014]. Moreover, as the BDBP data set starts in 1979, it was not possible to start at an earlier period (cf. the 1960 conditions used by *Polvani et al.* [2011]). Three year averages were used as the BDBP data set employs several more basic functions than SPARC to make a continuous time series, meaning that there is more interannual variability, and we did not want to bias the simulations to one phase of the quasi-biennial oscillation for instance. Further details on the data set formulation, as well as an in depth data set comparison are presented by *Hassler et al.* [2013].

We also analyze the 22 CMIP5 models that used the SPARC ozone data set (CMIP5-SPARC) using output from their historical simulations (1850–2005) [*Taylor et al*., 2012]. Those data have been previously analyzed in the context of their ozone depletion [*Eyring et al*., 2013], and the main purpose here is to put the CAM results in the context of a broader range of model simulations, rather than discuss the CMIP5 results in depth. Results are only analyzed for one ensemble member of these runs (r1i1p1) to avoid biasing the analysis to one model. In addition, we show some trends from measurements and reanalysis products to put the model results in the context of observed changes.

The CAM results are reported for the mean of the time slices after discarding the first 20 years of the simulations as spin-up. We use the time slice simulations to estimate the uncertainty in the mean response, indicating significance using the standard error from the 80 years of simulation used. Uncertainty estimates for the linear trends in the observations include the effect of any lag-1 autocorrelation of the residuals [*Santer et al*., 2000]. The significance of the trends and differences is shown at the 5% level (i.e., 95% confidence intervals) using a one-tailed *t* test, appropriate for austral spring where we are confident on the sign of the trends. Outside of austral spring, significance should be interpreted at the 10% level (i.e., a two-tailed test).

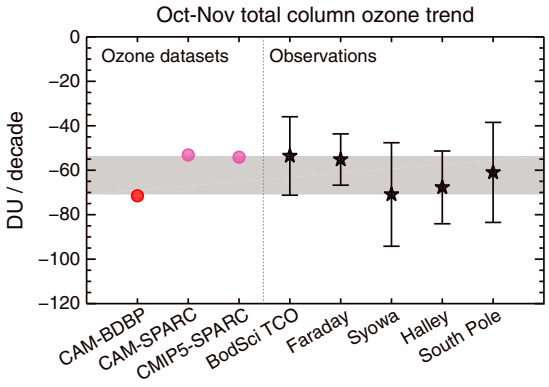

Figure 1. Changes in October–November average total column ozone (TCO) for the SH high latitudes (>65°S) over 1979–1997. Straight differences are shown for the CAM simulations (1995–1997 average minus 1979–1981 average), whereas linear trends are shown for the CMIP5-SPARC simulations and TCO observations. The BodSci TCO trend refers to version 2.8 of the Bodeker Scientific data set [*Struthers et al.*, 2009], which is based on combining several satellite measurements. The other observed trends are from several sites in Antarctica [see *Hassler et al.*, 2011]. The error bars for the observations indicate the 95% confidence intervals (one tail), and the gray shading indicates the observational range for the TCO trend, without error.

3. Climate Impact Versus Level of Ozone Depletion

Figure 1 compares the October–November total column ozone (TCO) change (CAM simulations) and trends (CMIP5-SPARC and observations) over 1979–1997, illustrating the strong ozone depletion over the SH high latitudes (>65°S) for this period [e.g., *Solomon*, 1999]. Excluding the uncertainty bars in the figure, the ozone changes used to force the CAM simulations bracket the estimates of the total column ozone depletion from the Bodeker Scientific observational data set [*Struthers et al.*, 2009] and several measurement sites [see *Hassler et al.*, 2011], with the BDBP data set having ~35% more ozone depletion than SPARC. The range of observed trend estimates reflects (in part) the eastward rotation of the polar vortex over this period, meaning that some sites on the edge of the continent have been sampling less (or more) vortex air [*Hassler et al.*, 2011]. The trends presented here have not been subsampled to include only vortex air. The ozone trend (i.e., from a linear least squares fit) for the CMIP5-SPARC simulations is nearly identical to the ozone change in the CAM-SPARC simulations (i.e., the difference between the ozone hole and preozone hole periods), indicative of the near linear ozone trend over this period in that data set and of the dominance of stratospheric ozone trends over tropospheric ozone trends. Additionally, there are differences in the trends between the two data sets at different altitudes [see *Hassler et al.*, 2013] that may be of additional importance for understanding the climate impacts, although this is not investigated here.

What does the relatively lower ozone loss in the SPARC data set mean for the climate impacts of ozone depletion? Figure 2 compares the SH high-latitude CMIP5-SPARC ensemble mean 1979–1997 trends in temperature, geopotential height, and zonal mean zonal wind against observations from radiosondes (temperature) and estimates from reanalysis fields (geopotential height and wind; see caption for details).

As is well known [e.g., *Thompson and Solomon*, 2002; *Perlwitz et al.*, 2008], the temperature trends are all characterized by strong stratospheric cooling around the time of the ozone hole (October–December) due to the reduction in radiative heating, which in turn is associated with strong negative trends in geopotential height that extend into the troposphere in austral summer, and a strengthening of the circumpolar winds. Acknowledging the uncertainty in the trends and the relatively short period over which they were calculated, Figure 2 does suggest that the ensemble mean CMIP5-SPARC trends are 30–50% weaker than those calculated from the radiosondes and reanalyses, at least for peak trends in the stratosphere. For instance, the observed cooling trends for November at 100 hPa are -4.2 ± 3.1 K/decade (RICH-obs) and -5.0 ± 3.3 K/decade (Iterative Universal Kriging (IUK)), compared to -3.0 ± 1.9 K/decade for CMIP5-SPARC; reanalysis geopotential height trends for November at 30 hPa are -182 ± 199 m/decade (Modern Era Retrospective-Analysis for Research and Applications (MERRA)) and -176 ± 191 m/decade (European Centre for Medium-Range Weather Forecasts Reanalysis (ERA-Interim)), compared to -126 ± 80 m/decade for CMIP5-SPARC; and reanalysis zonal mean zonal wind trends for December (peak month) at 100 hPa are 2.9 ± 2.1 ms^{-1}/decade (MERRA) and 2.2 ± 2.4 ms^{-1}/decade (ERA-Interim), compared to 1.0 ± 1.7 ms^{-1}/decade for CMIP5-SPARC. The intermodel spread (±1 standard deviation) is used to establish uncertainties for the CMIP5 trends, and for the radiosonde and reanalyses, they are estimated from the regression fit (the reanalysis trends are all significant at the 10% level, one-tailed test). We also note that despite all having identical levels of ozone depletion, individual CMIP5-SPARC models exhibit a range of different trends, with an interquartile range for 100 hPa November temperature trends of −4.0 to −2.6 K/decade. Of course, deficiencies in the models other

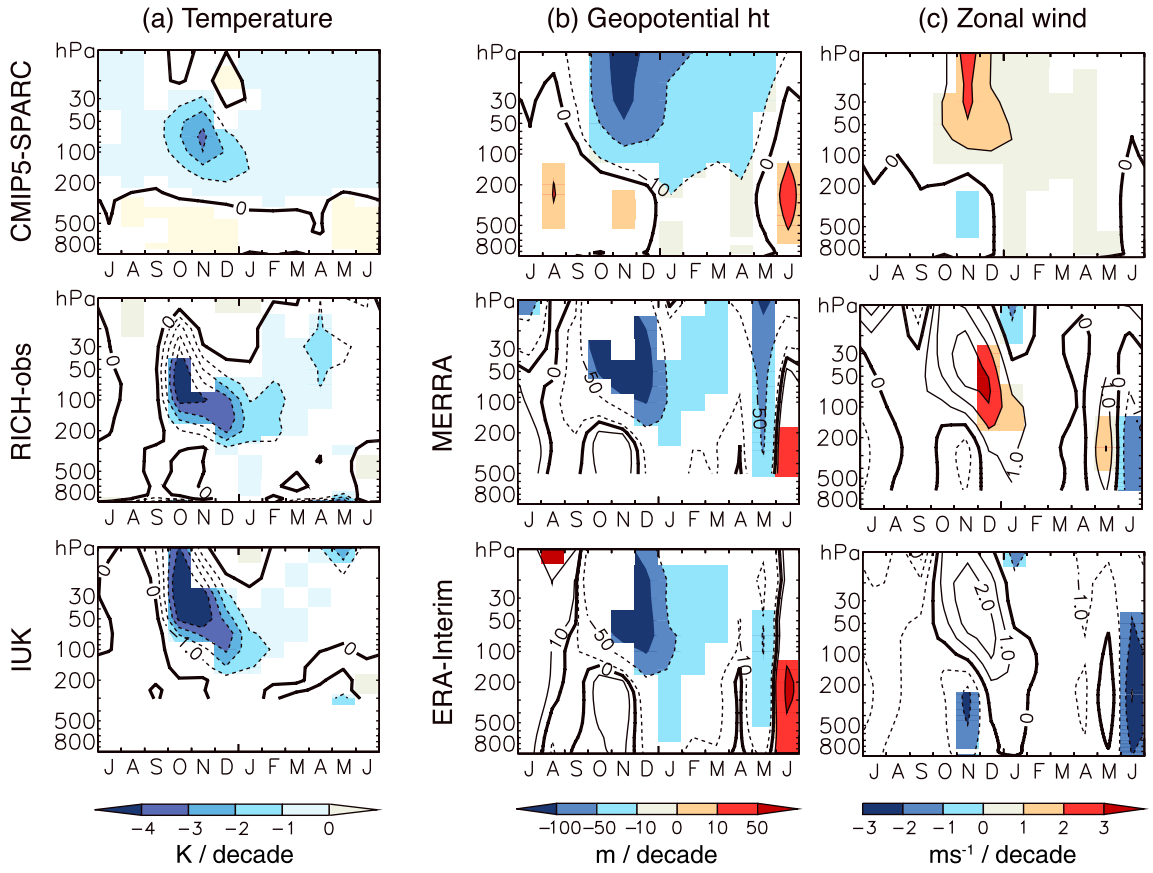

Figure 2. Altitude-month plots of the trend in (a) temperature (>65°S), (b) geopotential height (>65°S), and (c) zonal mean zonal wind (50°S–70°S) over 1979–1997 for the (top) CMIP5-SPARC simulations and (middle and bottom) observations and observationally based data sets. The observed temperature trends come from averaging the stations in the RICH-obs [*Haimberger et al.*, 2012] and IUK [*Sherwood et al.*, 2008] data sets in the region poleward of 65°S [see *Young et al.*, 2013a]. The reanalysis trends from the MERRA [*Rienecker et al.*, 2011] and ERA-Interim [*Dee et al.*, 2011] data sets are shown for geopotential height and zonal wind. The color-filled contours for CMIP5-SPARC indicate where the trend is significant at the 5% level (one tail), based on the spread of trends from the 22 climate models. For the other panels, the color-filled contours indicate where the trend is significant at the 5% level (one tail), based on the uncertainty in the linear regression.

than their level of ozone depletion could also be important in any discrepancy-compared observations, although it is likely that ozone depletion is the dominant driver of the cooling trend [*Gillett et al.*, 2011].

We turn next to the question of how different the climate impact of ozone depletion is between the SPARC (low-depletion estimate) and BDBP (high-depletion estimate) ozone data sets. Figure 3 shows the climate impacts of ozone depletion from these data sets in our CAM simulations, illustrating the effect on temperature, geopotential height, and zonal wind in a similar manner to Figure 2. Some additional climate impact metrics are presented in Table 1.

From Figure 3 and the stratospheric metrics in Table 1 (Z_{30} and T_{100}), it is immediately clear that the additional ~35% ozone depletion in the CAM-BDBP simulations results in much stronger austral spring SH high-latitude cooling and decreases in geopotential height and a stronger increase in the strength of the SH midlatitude zonal wind (associated with a jet shift, discussed below). In the stratosphere, the peak impacts are approximately doubled in the CAM-BDBP simulations compared to CAM-SPARC. In addition, the significant impacts in the CAM-BDBP simulations last for a longer part of the year and display larger impacts in the austral summer at lower altitudes. This may reflect the additional effects from the stronger cooling in these simulations, as well as a small level of additional ozone depletion outside of the ozone hole season in BDBP compared to SPARC (not shown).

As well as the stratospheric impact, Figure 3 shows the additional ozone depletion in the CAM-BDBP simulation results in stronger effects penetrating into the troposphere and with significant impacts persisting longer. For instance, the cooling trend penetrates more deeply into the troposphere with CAM-BDBP, due

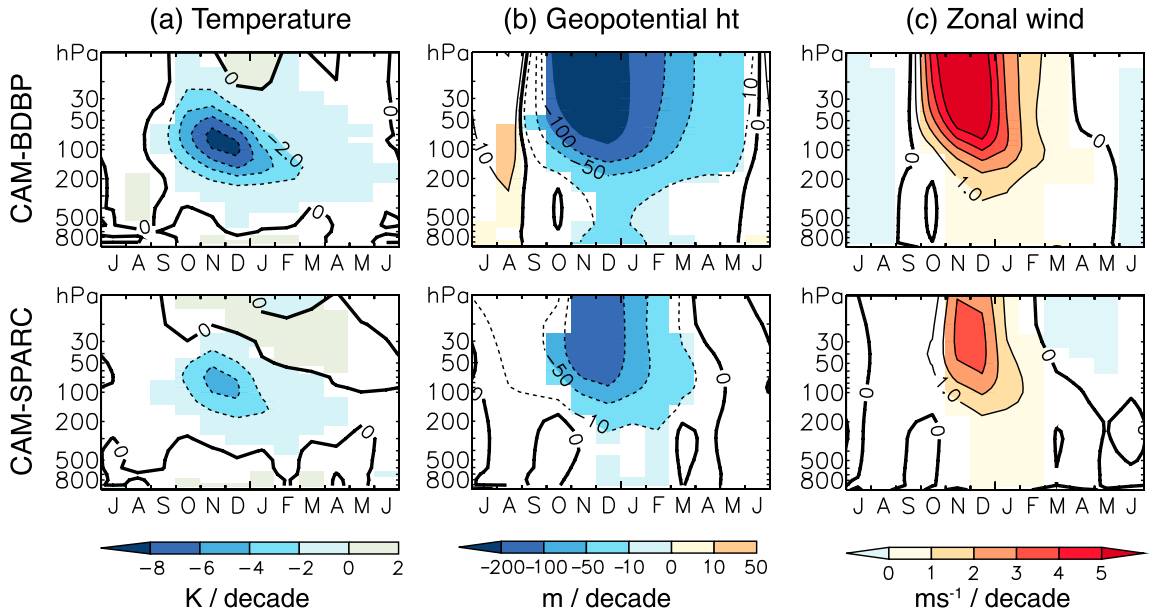

Figure 3. Altitude-month plots of the change in (a) temperature (>65°S), (b) geopotential height (>65°S), and (c) zonal mean zonal wind (50°S–70°S) between the ozone hole and preozone hole (top) CAM-BDBP and (bottom) CAM-SPARC simulations. The color-filled contours indicate where the change is significant at the 5% level (one tail), based on the interannual variability in the time slice simulations.

to the stronger radiatively induced temperature response from greater stratospheric cooling [*Grise et al.*, 2009]. In addition, the austral summer polar cap 500 hPa geopotential height trend for CAM-BDBP is nearly double that for CAM-SPARC (Table 1). Although not apparent from the contour in Figure 3, the austral summer tropospheric zonal wind impact is also 60–100% stronger in the CAM-BDBP simulations. These tropospheric circulation changes induced by ozone depletion are congruent with a trend toward a positive SAM index [*Thompson et al.*, 2011], and Table 1 shows that this is the case for CAM simulations. Here we show the austral summer trend in a SAM index defined using the difference between the zonal mean sea level pressure at 40°S and 65°S [*Gong and Wang*, 1999; *Gillett and Fyfe*, 2013], and the effect of the CAM-BDBP ozone depletion on this index is ~70% stronger than for the CAM-SPARC simulations. A positive SAM trend is also associated with a poleward migration of the midlatitude SH storm tracks [*Yin*, 2005], indicated in Table 1 by the shift in the latitude of zonal mean zonal wind in the lower troposphere (mean $u_{850\ hPa}$ [see *Davis and Rosenlof*, 2012]), which is 45% stronger in the CAM-BDBP simulations, related to a 50% larger increase in rainfall around 60°S (approximate location of peak rainfall, not shown). As others have noted, the tropospheric impacts of ozone depletion appear to extend into the SH subtropics [e.g., *Kang et al.*, 2011]. We find a similar result here, and Table 1 indicates that the poleward migration of the edge

Table 1. Impact of Ozone Depletion on a Range of Climate Metrics for the CAM-BDBP and CAM-SPARC Simulations[a]

	CAM-BDBP	CAM-SPARC
$Z_{30\ hPa}$ (>65°S, Nov)/m decade^{-1}	−315	−150
$T_{100\ hPa}$ (>65°S, Nov)/K decade^{-1}	−7.2	−3.5
$Z_{500\ hPa}$ (>65°S, December-January-February (DJF))/m decade^{-1}	−11.9	−6.6
SAM index[b] (DJF)/hPa decade^{-1}	1.2	0.7
Latitude of mean $u_{850\ hPa}$[c,d] (DJF)/deg decade^{-1}	0.42	0.29
Latitude where $\Psi_{500\ hPa}$[c,e] = 0 (DJF)/deg decade^{-1}	0.14	0.12

[a] All impacts are significant at the 5% level (one tail).
[b] Calculated from mean sea level pressure at 65°S and 40°S, following *Gong and Wang* [1999].
[c] Positive trend indicates south (poleward) shift.
[d] First moment of the area-weighted distribution of zonal mean zonal wind at 850 hPa (between 15°S and 70°S). See *Davis and Rosenlof* [2012].
[e] Where the stream function (Ψ) equals zero is indicative of the Hadley cell edge (e.g., *Johanson and Fu* [2009]).

of the SH Hadley cell—as determined by the latitude at which the zonal mean stream function equals zero [e.g., *Johanson and Fu*, 2009]—is larger in the CAM-BDBP simulations. However, we also note that the impact of the additional ozone depletion on this climate metric is more marginal than for the others discussed.

4. Discussion and Conclusions

Our CAM simulations show that varying ozone depletion within the uncertainty range estimated from observations results in clearly different climate impacts. The additional 35% ozone depletion in the CAM-BDBP simulations strengthens climate effects by ~100% in the stratosphere and by 20–100% in the troposphere. Previous multimodel analyses have demonstrated that models with stronger ozone depletion trends have stronger climate impacts [e.g., *Son et al*., 2010; *Eyring et al*., 2013], but none have explored the impact of different ozone depletion in the same model, using time slice experiments to isolate the climate signal. This is important since these are the types of experiments that are used to understand the climate fingerprint of ozone depletion, particularly when trying to attribute recent SH circulation changes between those driven by greenhouse gases and those driven by ozone changes [e.g., *Polvani et al*., 2011], even down to subcontinental scales [*Gonzalez et al*., 2013].

What this study has not done is to show that either ozone data set simulates a more faithful representation of late twentieth century climate change. Indeed, even though the CMIP5-SPARC ensemble mean trends are weaker than those estimated from observations and reanalyses, they are still within the uncertainty bounds and cannot be considered to be incorrect [see also *Young et al*., 2013a]. To explore this question more fully would require an ensemble of atmosphere-ocean climate model simulations forced with each data set that could then be compared against several observations. Moreover, completing such a set of simulations in more than one climate model would be important to explore the robustness of the result, something that is underlined by the range of trends from the CMIP-SPARC models, which all used the same ozone data set. However, both the SPARC and BDBP ozone data sets have their shortcomings [*Hassler et al*., 2013], and perhaps it is better for all climate model development to follow the lead of ~20% of current CMIP5 models [*Eyring et al*., 2013] and move to calculate ozone concentrations online, where the trends and distribution are at least dynamically consistent with the underlying climate model.

Overall, this study demonstrates that it is important for those analyzing climate/ozone links to be aware that varying the level of ozone depletion with the envelope of uncertainty described by the observations could lead to very different climate responses.

Acknowledgments

We would like to thank Jean-François Lamarque for his assistance in setting up CAM and Greg Bodeker of Bodeker Scientific for providing the combined total column ozone database. We acknowledge the World Climate Research Program's Working Group on Coupled Modeling, which is responsible for CMIP, and we thank the climate modeling groups for producing and making available their model output. For CMIP, the U.S. Department of Energy's Program for Climate Model Diagnosis and Intercomparison provides coordinating support and led the development of software infrastructure in partnership with the Global Organization for Earth System Science Portals. P.J.Y. acknowledges support of the Faculty of Science and Technology Research grant from Lancaster University. We also acknowledge the comments from two anonymous reviewers. Please contact the lead author to obtain the data and code used in this publication.

The Editor thanks two anonymous reviewers for their assistance in evaluating this paper.

References

Bandoro, J., S. Solomon, A. Donohoe, D. W. J. Thompson, and B. D. Santer (2014), Influences of the Antarctic ozone hole on Southern Hemispheric summer climate change, *J. Clim.*, *27*, 6245–6264, doi:10.1175/JCLI-D-13-00698.1.

Bodeker, G. E., B. Hassler, P. J. Young, and R. W. Portmann (2013), A vertically resolved, global, gap-free ozone database for assessing or constraining global climate model simulations, *Earth Syst. Sci. Data*, *5*, 31–43, doi:10.5194/essd-5-31-2013.

Chehade, W., M. Weber, and J. P. Burrows (2014), Total ozone trends and variability during 1979–2012 from merged data sets of various satellites, *Atmos. Chem. Phys.*, *14*(13), 7059–7074, doi:10.5194/acp-14-7059-2014.

Cionni, I., V. Eyring, J. F. Lamarque, W. J. Randel, D. S. Stevenson, F. Wu, G. E. Bodeker, T. G. Shepherd, D. T. Shindell, and D. W. Waugh (2011), Ozone database in support of CMIP5 simulations: Results and corresponding radiative forcing, *Atmos. Chem. Phys.*, *11*, 11,267–11,292, doi:10.5194/acp-11-11267-2011.

Collins, W. D., et al. (2006), The Community Climate System Model Version 3 (CCSM3), *J. Clim.*, *19*, 2122–2143, doi:10.1175/JCLI3761.1.

Davis, S. M., and K. H. Rosenlof (2012), A multi-diagnostic intercomparison of tropical width time series using reanalyses and satellite observations, *J. Clim.*, *25*, 1061–1078, doi:10.1175/JCLI-D-11-00127.1.

Dee, D. P., et al. (2011), The ERA-Interim reanalysis: Configuration and performance of the data assimilation system, *Q. J. R. Meteorol. Soc.*, *137*, 553–597, doi:10.1002/qj.828.

Eyring, V., et al. (2013), Long-term ozone changes and associated climate impacts in CMIP5 simulations, *J. Geophys. Res. Atmos.*, *108*, 5029–5060, doi:10.1002/jgrd.50316.

Gerber, E. P., and S.-W. Son (2014), Quantifying the summertime response of the austral jet stream and Hadley Cell to stratospheric ozone and greenhouse gases, *J. Clim.*, *27*, 5538–5559, doi:10.1175/JCLI-D-13-00539.1.

Gillett, N. P., and D. W. Thompson (2003), Simulation of recent Southern Hemisphere climate change, *Science*, *302*, 273–275, doi:10.1126/science.1087440.

Gillett, N. P., and J. C. Fyfe (2013), Annular mode changes in the CMIP5 simulations, *Geophys. Res. Lett.*, *40*, 1189–1193, doi:10.1002/grl.50249.

Gillett, N. P., J. F. Scinocca, D. A. Plummer, and M. C. Reader (2009), Sensitivity of climate to dynamically-consistent zonal asymmetries in ozone, *Geophys. Res. Lett.*, *36*, L10809, doi:10.1029/2009GL037246.

Gillett, N. P., et al. (2011), Attribution of observed changes in stratospheric ozone and temperature, *Atmos. Chem. Phys.*, *11*, 599–609, doi:10.5194/acp-11-599-2011.

Gong, D., and S. Wang (1999), Definition of Antarctic Oscillation index, *Geophys. Res. Lett.*, *26*, 459–462, doi:10.1029/1999GL900003.

Gonzalez, P. M., L. Polvani, R. Seager, and G. P. Correa (2013), Stratospheric ozone depletion: A key driver of recent precipitation trends in South Eastern South America, *Clim. Dyn.*, 1775–1792, doi:10.1007/s00382-013-1777-x.

Grise, K. M., D. W. Thompson, and P. M. Forster (2009), On the role of radiative processes in stratosphere–troposphere coupling, *J. Clim.*, *22*, 4154–4161, doi:10.1175/2009JCLI2756.1.

Haimberger, L., C. Tavolato, and S. Sperka (2012), Homogenization of the global radiosonde temperature dataset through combined comparison with reanalysis background series and neighboring stations, *J. Clim.*, *25*, 8108–8131, doi:10.1175/JCLI-D-11-00668.1.

Hassler, B., G. E. Bodeker, S. Solomon, and P. J. Young (2011), Changes in the polar vortex: Effects on Antarctic total ozone observations at various stations, *Geophys. Res. Lett.*, *38*, L01805, doi:10.1029/2010GL045542.

Hassler, B., P. J. Young, R. W. Portmann, G. E. Bodeker, J. S. Daniel, K. H. Rosenlof, and S. Solomon (2013), Comparison of three vertically resolved ozone data sets: Climatology, trends and radiative forcings, *Atmos. Chem. Phys.*, *13*, 5533–5550, doi:10.5194/acp-13-5533-2013.

Johanson, C. M., and Q. Fu (2009), Hadley cell widening: Model simulations versus observations, *J. Clim.*, *22*, 2713–2725, doi:10.1175/2008JCLI2620.1.

Kang, S. M., L. M. Polvani, J. C. Fyfe, and M. Sigmond (2011), Impact of polar ozone depletion on subtropical precipitation, *Science*, *332*, 951–954, doi:10.1126/science.1202131.

Logan, J. A. (1999), An analysis of ozonesonde data for the troposphere: Recommendations for testing 3-D models and development of a gridded climatology for tropospheric ozone, *J. Geophys. Res.*, *104*, 16,115–116,150, doi:10.1029/1998JD100096.

Manatsa, D., Y. Morioka, S. K. Behera, T. Yamagata, and C. H. Matarira (2013), Link between Antarctic ozone depletion and summer warming over southern Africa, *Nat. Geosci.*, *6*, 1–6, doi:10.1038/ngeo1968.

Mckenzie, R. L., P. J. Aucamp, A. F. Bais, L. O. Björn, M. Ilyas, and S. Madronich (2011), Ozone depletion and climate change: impacts on UV radiation, *Photochem. Photobiol. Sci.*, *10*, 182–198, doi:10.1039/c0pp90034f.

Perlwitz, J., S. Pawson, R. L. Fogt, J. E. Nielsen, and W. D. Neff (2008), Impact of stratospheric ozone hole recovery on Antarctic climate, *Geophys. Res. Lett.*, *35*, L08714, doi:10.1029/2008GL033317.

Polvani, L. M., D. W. Waugh, G. J. P. Correa, and S.-W. Son (2011), Stratospheric ozone depletion: The main driver of twentieth-century atmospheric circulation changes in the Southern Hemisphere, *J. Clim.*, *24*, 795–812, doi:10.1175/2010JCLI3772.1.

Randel, W. J., and F. Wu (2007), A stratospheric ozone profile data set for 1979–2005: Variability, trends, and comparisons with column ozone data, *J. Geophys. Res.*, *112*, D06313, doi:10.1029/2006JD007339.

Randel, W. J., R. R. Garcia, N. Calvo, and D. Marsh (2009), ENSO influence on zonal mean temperature and ozone in the tropical lower stratosphere, *Geophys. Res. Lett.*, *36*, L15822, doi:10.1029/2009GL039343.

Reinsel, G., E. C. Weatherhead, G. Tiao, A. Miller, R. Nagatani, D. J. Wuebbles, and L. Flynn (2002), On detection of turnaround and recovery in trend for ozone, *J. Geophys. Res.*, *107*, 4078, doi:10.1029/2001JD000500.

Rienecker, M. M., et al. (2011), MERRA - NASA's Modern-Era Retrospective Analysis for Research and Applications, *J. Clim.*, *24*, 3624–3648, doi:10.1175/JCLI-D-11-00015.1.

Santer, B. D., T. M. L. Wigley, J. S. Boyle, D. J. Gaffen, J. J. Hnilo, D. Nychka, D. E. Parker, and K. E. Taylor (2000), Statistical significance of trends and trend differences in layer-average atmospheric temperature time series, *J. Geophys. Res.*, *105*, 7337–7356, doi:10.1029/1999JD901105.

Seviour, W. J. M., S. C. Hardiman, L. J. Gray, N. Butchart, C. MacLachlan, and A. A. Scaife (2014), Skillful seasonal prediction of the Southern Annular Mode and Antarctic ozone, *J. Clim.*, *27*, 7462–7474, doi:10.1175/JCLI-D-14-00264.1.

Sherwood, S. C., C. L. Meyer, R. J. Allen, and H. A. Titchner (2008), Robust tropospheric warming revealed by iteratively homogenized radiosonde data, *J. Clim.*, *21*, 5336–5352, doi:10.1175/2008JCLI2320.1.

Shindell, D., G. Faluvegi, L. Nazarenko, K. Bowman, J.-F. Lamarque, A. Voulgarakis, G. A. Schmidt, O. Pechony, and R. Ruedy (2013), Attribution of historical ozone forcing to anthropogenic emissions, *Nat. Clim. Change*, *3*, 567–570, doi:10.1038/nclimate1835.

Solomon, S. (1999), Stratospheric ozone depletion: A review of concepts and history, *Rev. Geophys.*, *37*, 275–316, doi:10.1029/1999RG900008.

Solomon, S., P. J. Young, and B. Hassler (2012), Uncertainties in the evolution of stratospheric ozone and implications for recent temperature changes in the tropical lower stratosphere, *Geophys. Res. Lett.*, *39*, L17706, doi:10.1029/2012GL052723.

Son, S.-W., N. F. Tandon, L. M. Polvani, and D. W. Waugh (2009), Ozone hole and Southern Hemisphere climate change, *Geophys. Res. Lett.*, *36*, L15705, doi:10.1029/2009GL038671.

Son, S.-W., et al. (2010), Impact of stratospheric ozone on Southern Hemisphere circulation change: A multimodel assessment, *J. Geophys. Res.*, *115*, D00M07, doi:10.1029/2010JD014271.

Son, S.-W., A. Purich, H. H. Hendon, B.-M. Kim, and L. M. Polvani (2013), Improved seasonal forecast using ozone hole variability?, *Geophys. Res. Lett.*, *40*, 6231–6235, doi:10.1002/2013GL057731.

Struthers, H., et al. (2009), The simulation of the Antarctic ozone hole by chemistry-climate models, *Atmos. Chem. Phys.*, *9*, 6363–6376, doi:10.5194/acp-9-6363-2009.

Taylor, K. E., R. J. Stouffer, and G. A. Meehl (2012), An overview of CMIP5 and the experiment design, *Bull. Am. Meteorol. Soc.*, *93*, 485–498, doi:10.1175/BAMS-D-11-00094.1.

Thompson, D. W. J., and S. Solomon (2002), Interpretation of recent Southern Hemisphere climate change, *Science*, *296*, 895–899, doi:10.1126/science.1069270.

Thompson, D. W. J., S. Solomon, P. J. Kushner, M. H. England, K. M. Grise, and D. J. Karoly (2011), Signatures of the Antarctic ozone hole in Southern Hemisphere surface climate change, *Nat. Geosci.*, *4*, 741–749, doi:10.1038/ngeo1296.

Yin, J. H. (2005), A consistent poleward shift of the storm tracks in simulations of 21st century climate, *Geophys. Res. Lett.*, *32*, L18701, doi:10.1029/2005GL023684.

Young, P. J., A. H. Butler, N. Calvo, L. Haimberger, P. J. Kushner, D. R. Marsh, W. J. Randel, and K. H. Rosenlof (2013a), Agreement in late twentieth century Southern Hemisphere stratospheric temperature trends in observations and CCMVal-2, CMIP3 and CMIP5 models, *J. Geophys. Res. Atmos.*, *118*, 605–613, doi:10.1002/jgrd.50126.

Young, P. J., et al. (2013b), Pre-industrial to end 21st century projections of tropospheric ozone from the Atmospheric Chemistry and Climate Model Intercomparison Project (ACCMIP), *Atmos. Chem. Phys.*, *13*, 2063–2090, doi:10.5194/acp-13-2063-2013.